MRI based knee cartilage assessment

Dirk - Jan Kroon[a] and Przemyslaw Kowalski[a] and Wojciech Tekieli[a] and Els Reeuwijk[b] and Daniel Saris[a,c] and Cornelis H. Sump[a]

[a]MIRA Institute for Biomedical Technology and Technical Medicine, University of Twente, Enschede, the Netherlands;
[b]Experimental Center for Technical Medicine, University of Twente, Enschede, the Netherlands;
[c]Dept. of Orthopedics, University Medical Center Utrecht, Utrecht, the Netherlands;

ABSTRACT

Osteoarthritis is one of the leading causes of pain and disability worldwide and a major health problem in developed countries due to the gradually aging population. Though the symptoms are easily recognized and described by a patient, it is difficult to assess the level of damage or loss of articular cartilage quantitatively. We present a novel method for fully automated knee cartilage thickness measurement and subsequent assessment of the knee joint. First, the point correspondence between a pre-segmented training bone model is obtained with use of Shape Context based non-rigid surface registration. Then, a single Active Shape Model (ASM) is used to segment both Femur and Tibia bone. The surfaces obtained are processed to extract the Bone-Cartilage Interface (BCI) points, where the proper segmentation of cartilage begins. For this purpose, the cartilage ASM is trained with cartilage edge positions expressed in 1D coordinates at the normals in the BCI points. The whole cartilage model is then constructed from the segmentations obtained in the previous step. An absolute thickness of the segmented cartilage is measured and compared to the mean of all training datasets, giving as a result the relative thickness value. The resulting cartilage structure is visualized and related to the segmented bone. In this way the condition of the cartilage is assessed over the surface. The quality of bone and cartilage segmentation is validated and the Dice's coefficients 0.92 and 0.86 for Femur and Tibia bones and 0.45 and 0.34 for respective cartilages are obtained. The clinical diagnostic relevance of the obtained thickness mapping is being evaluated retrospectively. We hope to validate it prospectively for prediction of clinical outcome the methods require improvements in accuracy and robustness.

Keywords: Cartilage segmentation, bone segmentation, Active Shape Models, Active Appearance Models, knee joint, thickness mapping

1. INTRODUCTION

Osteoarthritis (OA) is a clinical syndrome of joint pain, accompanied by functional limitations and reduced quality of life.[1] Sociologically, it is one of the leading causes of pain and disability worldwide.[1] It is one of the major health problems in developed countries, due to the gradually aging population.[2] OA is a complex metabolic problem, it affects all joint tissues (including cartilage, ligaments, muscle and bone,[1] and can affect all the joints (with emphasis put on knee, hip and hands[1]). As the widespread symptoms are easily recognized and described by a patient, it is difficult to infer and assess the level of disorder quantitatively. As the damage and / or loss of articular cartilage is the most objective proof of OA amongst other symptoms, the overall state of the joint is usually described by the state of the cartilage itself, see Fig.1. The imaging modality of choice is MRI because it uses no ionizing radiation which makes the technique ideal for longitudinal studies. Quantitative analysis of the cartilage holds a crucial role in the process of diagnosis of this increasingly common disease,[3] requiring a robust method of disease-stage analysis. This is mainly because the process of manual segmentation / assessment of cartilage is tedious and time - consuming, and also the outcome may vary depending on the observer. As cartilage does not corresponds to a specific intensity on MRI, the research effort has to be put on automated segmentation, see Fig. 2.

Further author information: (Send correspondence to C.H.S.)
C.H.S.: E-mail: c.h.slump@utwente.nl, Telephone: +31 (0)53 4892094

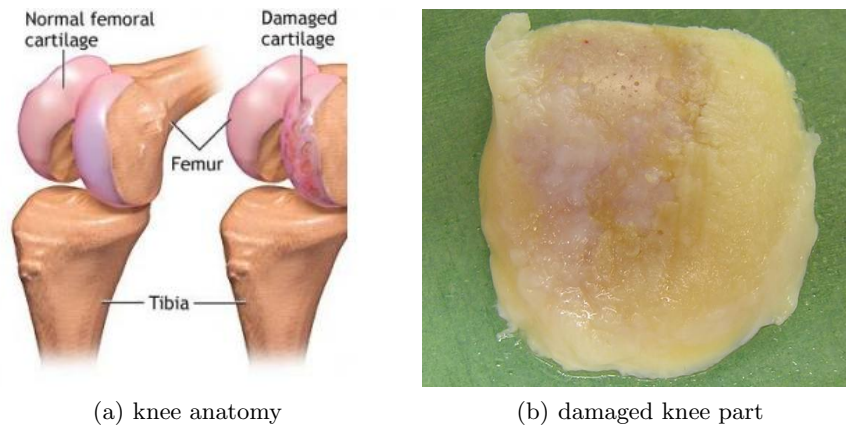(a) knee anatomy   (b) damaged knee part

Figure 1. On the left (a) part of the normal knee anatomy and the knee anatomy with indicated damaged cartilage. On the right (b) a surgical removed part of the knee, showing the damaged cartilage.

Figure 2. Example of an MRI showing the cross section of a normal knee, note that the cartilage does not show up with a different intensity.

This problem has been recognized and a so - called grand challenge was devoted to this task at the "Medical Image Analysis for the Clinic: A Grand Challenge" workshop at 2010 Medical Image Computing and Computer Assisted Intervention (MICCAI) conference in Beijing, China.[2] Several approaches are described in the 2010 MICCAI proceedings. The fully - automatic algorithms utilize the Active Shape Models (ASM's)[4] as well as Active Appearance Models (AAM's),[5] introduced by [6] to segment the Tibial and Femoral bones within the knee joint. To segment the cartilage afterwards, techniques as multi - object segmentation[4] or region growing starting from the bone surface are incorporated. Also uniform solutions for both bone and cartilage extraction, including *e.g* graph - cuts method[7,8] or statistical deformation models,[9] are described. Though from an application point - of - view, the fully - automatic methods are the most comfortable in use, they may not lead to the best obtainable results. Semi - automatic methods[10,11] can be used in this case. Requiring more user interaction during the segmentation process (the user marks the points where the segmentation of appropriate structures should begin), they may (but not have to) lead to more acceptable and precise outcomes. Some of the semi-automatic methods may also require the user to interact in the end of segmentation process, to delete some false-positive extractions.[3] The current paper present a novel method for fully automated knee cartilage thickness measurement and subsequent assessment of the knee joint. The method is described in detail in the next section, the section hereafter contains the (preliminary) results and a discussion.

2. MATERIALS AND METHODS

The proposed system is depicted in Figure 3 and consists of two major parts, *i.e.* training and testing. With testing we mean the comparison of the results of the method with a so - called groundtruth. Before MRI images

of the knee can be processed in order to assess the joint, the algorithms for bone and cartilage segmentation are first trained based upon supplied data, labeled by an expert.

2.1 Image data

The image data we train our method with, is provided by the MICCAI 2010 Grand Challenge (WWW.SKI10.ORG), mentioned in the introduction. According to the organizers[2] of the SKI10 challenge, the knee MRI images originate from the surgical planning program of Biomet, Inc. Cases of left and right knees are distributed approximately equally. Many centers in the USA have contributed to the data, using machines from all major vendors. All images were acquired in the sagittal plane with a pixel spacing of $0.39 \times 0.39mm$ and a slice distance of $1mm$. No contrast agents were used. Field strength was $1.5T$ in about 90% of the cases, the rest was acquired mostly at $3T$, with some images acquired at $1T$. The employed MRI sequences show a huge variety: the vast majority of images used T1-weighting, but some were also acquired with T2-weighting. Many images used gradient echo or spoiled gradient echo sequences, and fat suppression techniques were common as well. After acquisition, all images were segmented interactively by experts at Biomet, Inc. Structures of interest were femur, femoral cartilage, tibia, and tibial cartilage. As a special nicety to keep in mind, the organizers[2] state that as all images were used for surgery planning of partial or complete knee replacement, segmentations were created for a specific clinical goal, and that therefore the accuracy of the contours is varying. In areas where implant position guides should be placed, the accuracy of bone and cartilage segmentations is very high. In areas where the exact boundary of the cartilage to the sides is not relevant for the planned surgery, the provided contour may be quite far off the true location.

2.2 Algorithm

In this subsection we describe the various steps of the method and the details of the segmentation algorithm.

2.2.1 ASM Bone

The ASM bone training is based on the expert labeling of the Femur and Tibia in MRI images. The scans are not uniformly sampled, therefore we re-sample the scans and labels to a voxel resolution of $0.39 \times 0.39 \times 0.39]mm$, using cubic interpolation for the MRI data and nearest neighbor interpolation for the label data.

The first step in our algorithm is to subtract the ISO-surfaces of the regions labeled as Femur and Tibia using the marching cubes algorithm.

We want to use the vertices of the bone surfaces to train active shape models for both bones. Therefore all surfaces must contain an equal number of vertices, and every vertex must have a corresponding vertex in all surface descriptions at relatively the same location. To obtain the correspondences we non - rigidly register the surface geometry from one scan to all other surfaces. To capture the relative location of a vertex of the surface, we use 3D Shape Context[12] as feature. 3D Shape Context is an extension of the original Shape Context,[13] which describes every point on a (2D) figure by the vectors connecting that point with all other points within the shape. The vectors are represented by the log - distance r and the polar angle θ. Because this description (including all the points within the figure) is far too complex and too detailed, the number of vectors needs to be reduced. This is achieved by generating the coarse histogram (the actual shape context) of a particular point, which contains a pre - defined number of bins uniformly distributed in log - polar space, each filled with a number of points. The log - distance itself is also limited to an appropriate threshold. This makes the descriptor more sensitive to positions of nearby points, and neglects the influence of points that are farther than the chosen threshold distance. The histograms represented as vectors are called the feature vectors of the corresponding points. Matching costs $C(p,q)$ of the points p and q with histograms h_i and h_j, respectively, on two different shapes (described in K bins) can be measured:

$$C(p,q) = \frac{1}{2} \sum_{k=1}^{K} \frac{(h_i(k) - h_j(k))^2}{h_i(k) + h_j(k)}.$$

(1)

In this way, the matrix containing costs between each pair of points is generated. The optimal point - to - point matching is then defined as the one with a lowest total connection costs between the points. This matching is
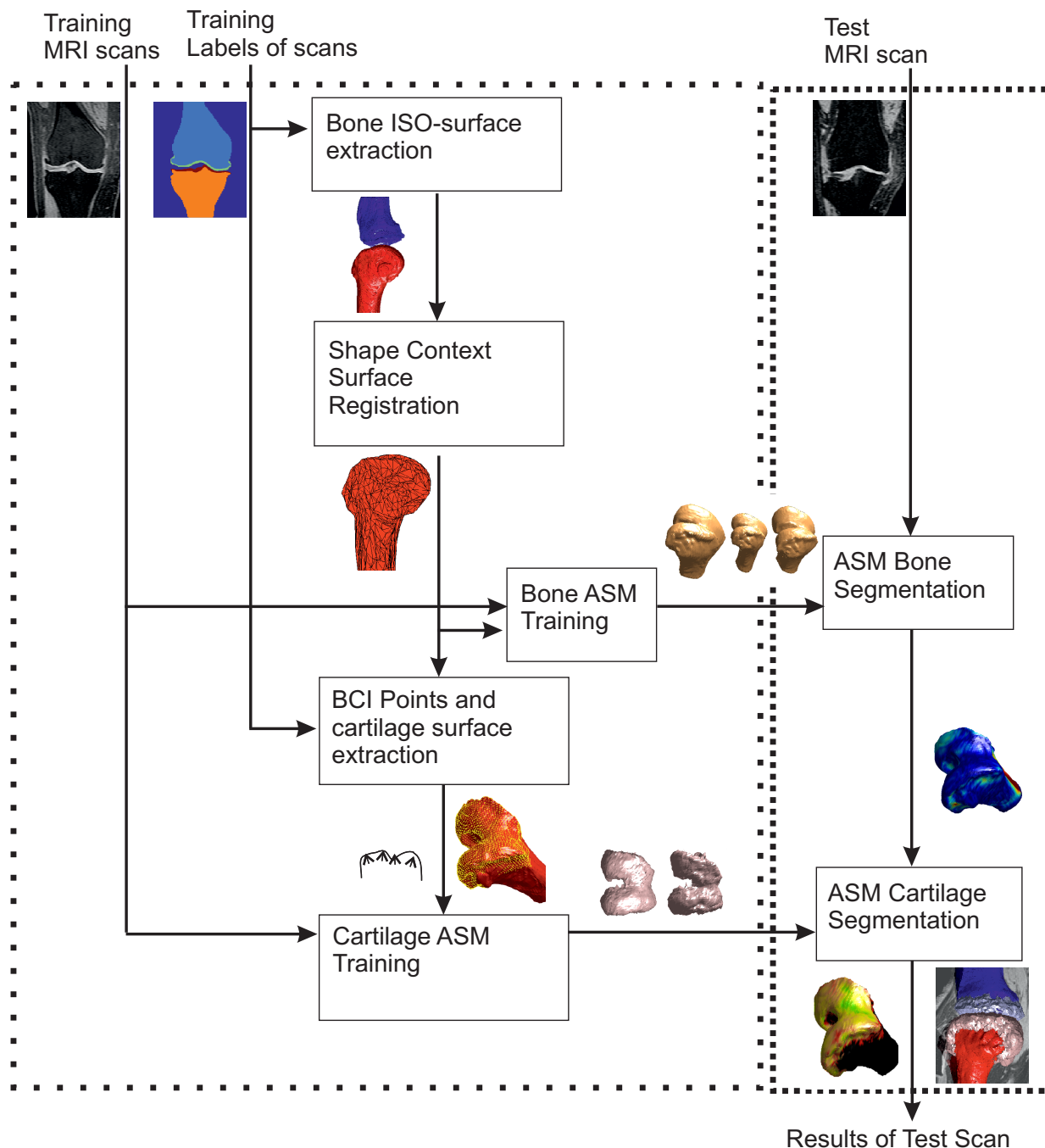
Figure 3. Scheme of the proposed knee cartilage assessment. The left - hand side shows the training of the Active Shape Model (ASM) for bone and cartilage. At the right - hand side the ASMs are used for the bone and cartilage segmentation.

obtained using a modification of the original Hungarian algorithm,[14] as will be described below. Because the MRI datasets of a knee are three - dimensional, the extension of the shape context method to 3D is necessary,[15] replacing the 2D log - polar histogram is replaced by a 3D log - spherical histogram, adding one more parameter to each of the particular vectors describing the shape context of each point. Because the uniform sampling of the azimuth and inclination (polar angle) within the spherical coordinate system will not result in a uniformly

distributed histogram, the inclination was therefore replaced with its cosine.[15] The transformation from the (x, y, z) coordinates of a point with radius r to the histogram coordinate system (o_r, o_θ, o_ϕ), is expressed by:

$$o_r = \frac{n_r}{log(r_{max}) - log(r_{min})} log(\frac{r}{r_{min}}) \tag{2}$$

$$o_\theta = n_\theta \frac{z}{r} \tag{3}$$

$$o_\phi = \frac{n_\phi}{2\pi} \arctan(\frac{y}{x}) \tag{4}$$

with n_r, n_θ and n_ϕ the number of histogram bins for each coordinate, and r_{max} and r_{min} corresponding to the maximum and minimum distance considered in the 3D shape. In brief, shape context captures the location of a point in relation to all other points using a histogram with on the x-axis the distance to a point and on the y-axis and z-axis the longitude/latitude angle relative to that point.

The registration works as follows. First we pick one bone surface as master which we register to a surface of another scan. We then calculate the 3D shape context feature descriptor for all points in both surface geometries. Then for every point in the master surface, we search for a point in the second surface with the minimum feature-distance, and also from the other surface to the master. These obtained point correspondences are then used to construct a B-spline grid which warps the master surface to the shape of the other surface. We repeat this procedure while refining the B-spline grid from rough to fine to get robust multi scale registration. After this procedure the master surface is transformed into the shape of the other surface, thus gives us corresponding points. Because we match points to points the transformed surface is in some regions still a pixel off from the real boundary. Therefore we use a modified iterative closest point (ICP) algorithm based on a distance transform, which calculates vectors from the vertices to the closest surface. We use these vectors to update the B-spline grid.

2.2.2 ASM Cartilage

After applying ASM bone segmentation on an MRI scan we obtain the location of the bone described by a surface geometry of vertices and faces. The cartilage is attached to the bone, thus if we sample intensities along the normals of surface vertices, we sample through the cartilage layer.

During shape context ASM bone building we obtain the bone surface geometry of all training scans. In the training scans we sample the intensities along the normals in the MRI data and also in the label volume. If we sample intensities for a certain vertex, and two or more test scans contain the cartilage label, we add this vertex to a set of bone cartilage interface (BCI) vertices.

For all BCI vertices we search along the vertex normal for the position of the cartilage - background edge. We use these 1D positions and MRI intensities on the normal around the position to train an ASM model for the cartilage.

During cartilage segmentation, we can simply sample long intensity profiles along the normals of the BCI vertices from the bone segmented by the ASM. We can then search along the long intensity profile for the part with matches the cartilage-background edge of the training data. Then we regularize the found 1D edge positions with the shape model of the cartilage ASM. The regularized 1D positions of the cartilage correspond to the cartilage thickness and can easily be re-mapped to 3D x, y, z positions.

3. RESULTS AND DISCUSSION

In this section we present preliminary results of our proposed method based upon the training on datasets $1-30$. After training the ASM bone model, we apply it to segment the bones in datasets $31-60$, see Fig. 4 for an example of dataset 35. We measure the performance by the Dice coefficient, which gives a value for the overlap between expert and model segmentation. The shaft of the bones are only partly present in the training data, therefore we only calculate the Dice coefficient for the part of the bones close to the knee joint. The results on datasets $31-60$ are shown in the left columns of Table 1. For the Tibia we obtain a mean Dice coefficient of

0.86 with a standard deviation of 0.12. For the Femur we obtain a mean Dice coefficient of 0.92 with a standard deviation of 0.05. For some data sets the initial bone model was not close enough to the bone in the image, leading to a few outliers with Dice coefficient near to 0.60. This can be prevented by doing a few iterations for several initial pose parameters and choosing the pose in which the distance between non-regularized shape and ASM regularized shape is the smallest.
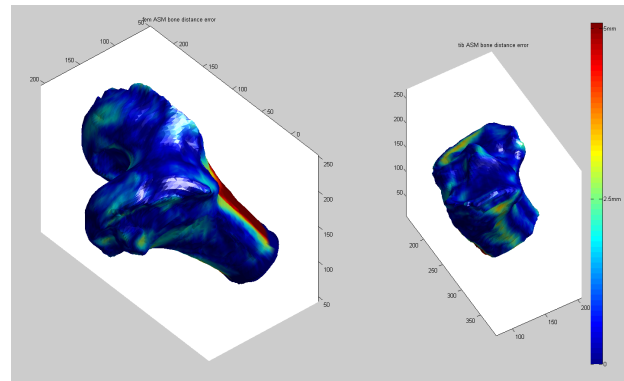

Figure 4. The distance error in the bone segmentation between the ASM and the expert of dataset 35.

After ASM bone segmentation we have sampled the intensities on the BCI normals, see Fig. 5 for the BCI points of the example of dataset 35 and have used the thus obtained profiles as input for our 1D ASM cartilage segmentation. The obtained cartilage of dataset 35 is shown in Fig. 6, as example, and compared with the
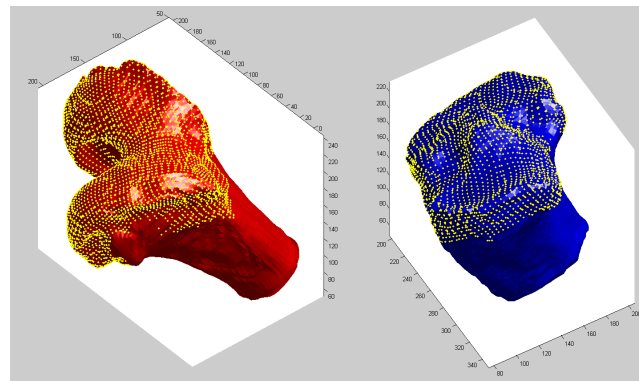

Figure 5. The obtained BCI points after the ASM bone segmentation for dataset 35.

expert's result. The results for datasets $31 - 60$ are shown in the right columns of Table 1. For the Tibia cartilage we obtain a mean Dice coefficient of 0.34 with a standard deviation of 0.09. For the Femur cartilage we obtain a mean Dice coefficient of 0.45 with a standard deviation of 0.09. The cartilage is on most BCI sites only a few voxels thick. Thus a small ASM bone segmentation error only leads already to a low cartilage Dice coefficient. Also the medical experts must have used learned shaped information to segment the cartilage when the cartilage background edge was not visible. An ASM model trains on all data also if no edge is visible. This leads to a trained search model which gives unreliable results. It would be better if the model training and segmentation included reliable weights related to edge visibility.

We also have measured the thickness in millimeter for the BCI points, and have compared the thickness between the manual expert and ASM segmentation, respectively. For dataset 35 the obtained cartilage thickness is shown and compared with the expert annotation in Fig. 7. The results for datasets $31 - 60$ are shown in Table 2. For the Tibia cartilage the mean average distance between model and expert segmentation is $1.09mm$.

Table 1. ASM bone and cartilage segmentation results measured by Dice overlap coefficient.

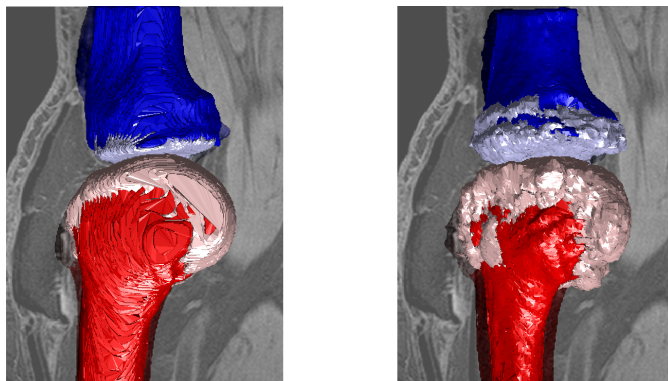|	ASM segmentation			
	Bone		Cartilage	
Id	Tibia	Femur	Tibia	Femur
31	0.54	0.79	0.15	0.25
32	0.92	0.96	0.48	0.43
33	0.95	0.96	0.43	0.57
34	0.87	0.93	0.30	0.44
35	0.92	0.90	0.43	0.53
36	0.90	0.94	0.43	0.54
37	0.94	0.81	0.30	0.31
38	0.84	0.95	0.29	0.59
39	0.89	0.90	0.26	0.47
40	0.64	0.79	0.22	0.30
41	0.94	0.95	0.32	0.47
42	0.72	0.88	0.25	0.49
43	0.66	0.95	0.36	0.52
44	0.94	0.95	0.41	0.54
45	0.93	0.92	0.43	0.44
46	0.94	0.95	0.36	0.45
47	0.84	0.95	0.36	0.59
48	0.93	0.95	0.33	0.42
49	0.61	0.92	0.12	0.30
50	0.93	0.94	0.37	0.49
51	0.86	0.96	0.31	0.52
52	0.93	0.91	0.44	0.44
53	0.89	0.93	0.44	0.47
54	0.95	0.94	0.30	0.31
55	0.93	0.94	0.36	0.50
56	0.95	0.95	0.46	0.53
57	0.75	0.82	0.28	0.31
58	0.95	0.95	0.38	0.43
59	0.95	0.95	0.33	0.44
60	0.63	0.90	0.32	0.43

Figure 6. The obtained cartilage with the ASM segmentation for dataset 35 on the right and the expert segmentation on the left.
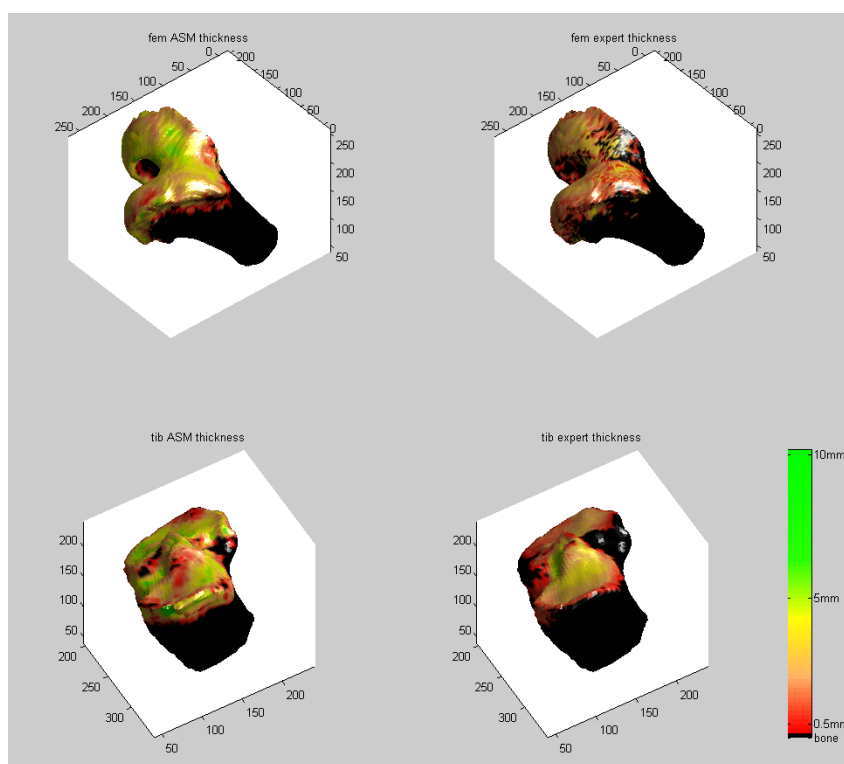

Figure 7. The cartilage thickness, comparison ASM segmentation with the expert, for dataset 35.

For the Femur the mean average distance is $1.39mm$. If we look at these mean distances values and results, we see that our model over - estimates the thickness of the cartilage. Of course we can subtract $1.1mm$ from our ASM cartilage segmentation, leading to much better results and higher Dice coefficients. But the values of the standard deviation and the maximum distance indicate that reliably results, are only to be obtained if we really improve the robustness of the ASM training algorithm.

The full results of our proposed method will appear on the website of the MICCAI 2010 Grand Challenge: WWW.SKI10.ORG, to where we have submitted the results on the provided 50 test datasets, after having trained the algorithm on the provided 60 annotated datasets.

Table 2. Difference in thickness (mm) between the ASM model and the expert segmentation, on BCI points of Tibial cartilage and Femural cartilage, respectively.

Difference in cartilage thickness (mm)					
	Tibia			Femur		
Id	mean	std	max	mean	std	max
31	1.00	1.94	6.89	1.44	1.94	9.96
32	0.60	1.41	6.12	1.62	1.74	12.29
33	1.06	1.39	7.31	1.28	1.63	12.92
34	1.38	1.52	7.11	1.54	1.55	10.26
35	1.16	1.65	9.39	1.37	1.66	11.37
36	0.93	1.77	8.26	1.48	1.63	12.19
37	1.44	1.33	9.79	1.85	1.86	12.41
38	0.01	1.87	5.65	0.42	2.16	12.95
39	1.10	1.54	8.32	1.23	1.84	12.28
40	1.22	1.67	8.31	1.64	1.69	13.75
41	1.25	1.43	7.00	1.18	1.64	14.34
42	0.99	1.60	8.18	1.63	1.84	11.61
43	1.10	1.59	8.67	1.18	1.72	13.32
44	0.64	1.66	7.51	0.86	1.89	10.42
45	1.08	1.36	8.15	1.29	1.69	9.75
46	1.07	1.38	7.08	1.27	1.55	9.99
47	1.26	1.48	8.55	0.97	1.77	9.33
48	1.32	1.43	8.07	1.70	1.70	12.97
49	1.35	1.67	9.23	1.85	1.75	11.69
50	1.41	1.31	7.18	1.55	1.66	11.12
51	0.95	1.49	9.46	1.17	1.67	10.64
52	1.32	1.47	7.99	1.59	1.69	14.48
53	0.99	1.40	6.79	1.33	1.57	10.82
54	1.43	1.34	8.16	1.62	1.62	11.15
55	1.17	1.43	9.19	1.36	1.64	14.34
56	1.08	1.44	6.84	1.29	1.71	14.11
57	1.16	1.41	7.87	1.25	1.87	11.61
58	1.05	1.51	7.66	1.56	1.71	11.19
59	1.09	1.43	8.52	1.61	1.69	12.02
60	1.11	1.59	7.61	1.45	1.79	15.37

REFERENCES

[1] [*The National Collaborating Centre for Chronic Conditions: Osteoarthritis, National clinical guideline for care and management in adults*], Royal College of Physicians, London (2008).

[2] Heimann, T., Morrison, B., Styner, M., Niethammer, M., and Warfield, S., "Segmentation of knee images: A grand challenge," in [*International Conference on Medical Image Computing and Computer Assisted Intervention (MICCAI)*], 207–214 (2010).

[3] Tamez-Pena, J. G., Barbu-McInnis, M., and Totterman, S., "Knee cartilage extraction and bone - cartilage interface analysis from 3D MRI data sets," in [*Medical Imaging: Image Processing*], J. M. Fitzpatrick, M. S., ed., *Proc. SPIE* **5370**, 1774–1784 (2004).

[4] Seim, H., Kainmueller, D., Lamecker, H., Bindernagel, M., Malinowski, J., and Zachow, S., "Model-based auto-segmentation of knee bones and cartilage in mri data," in [*International Conference on Medical Image Computing and Computer Assisted Intervention (MICCAI)*], 215–223 (2010).

[5] Vincent, G., Wolstenholme, C., Scott, I., and Bowes, M., "Fully automatic segmentation of the knee joint using active appearance models," in [*International Conference on Medical Image Computing and Computer Assisted Intervention (MICCAI)*], 224–230 (2010).

[6] Cootes, T. F. and Taylor, C. J., [*Statistical Models of Appearance for Computer Vision*], Technical Report, University of Manchester (March 2004). http://www.isbe.man.ac.uk.

[7] Lee, S., Shim, H., Park, S. H., Yun, I. D., and Lee, S. U., "Learning local shape and appearance for sebmentation of knee cartilage in 3d mri," in [*International Conference on Medical Image Computing and Computer Assisted Intervention (MICCAI)*], 231–240 (2010).

[8] Park, S. H., Lee, S., Yun, I. D., and Lee, S. U., "Automatic bone segmentation in knee magnetic resonance images using a coarse - to - fine strategy," in [*Medical Imaging: Image Processing*], Haynor, D. R. and Ourselin, S., eds., *Proc. SPIE* **8314** (2012).

[9] Amberg, M., Lüthi, M., and Vetter, T., "Fully automatic segmentation of the knee using local deformation - model fitting," in [*International Conference on Medical Image Computing and Computer Assisted Intervention (MICCAI)*], 251–260 (2010).

[10] Eckstein, F., Gavazzeni, A., Sittek, H., Hauber, M., Lösch, A., Englmeier, K.-H., Schulte, E., Putz, R., and Reiser, M., "Determination of knee joint cartilage thickness using three - dimensional magnetic resonance chondro crassometry," *Magnetic Resonance in Medicine* **36**, 256–265 (2005).

[11] Kitney, R. I., Cashman, P. M. M., and Carter, M. E., "Fast automated segmentation and visualization methods for MR images of the knee joint in arthritis," in [*Proceedings of the 20th Anual International Conference of the IEEE EMBS*], **20**, 559–562 (1998).

[12] Kroon, D. J., "Shape context based corresponding point models," in [*MATLAB Central File Exchange*],

[13] Belongie, S., Malik, J., and Puzicha, J., "Shape matching and object recognition using shape contexts," *IEEE Trans. PAMI* **24**, 509–522 (2002).

[14] Munkres, J., "Algorithms for the assignment and transportation problems," *J. SIAM.* **5**, 32–38 (1957).

[15] Kroon, D. J., [*Segmentation of the Mandibular Canal in Cone-Beam CT Data*], PhD thesis, University of Twente, Enschede, the Netherlands (December 2011).